Int. J. Electrochem. Sci., 12 **(2017)** 1808 – 1817, doi: 10.20964/2017.03.35

International Journal of
ELECTROCHEMICAL
SCIENCE
www.electrochemsci.org

Electrochemical Performance of Chitosan Oligosaccharide/Carbon Nanotube Composite for Detection of Trace Copper(II) Ion

Tingkai Zhao, Xianglin Ji, Wenbo Jin, Shasha Guo, Yuanbo Cheng, Xuan Wang,*
Alei Dang, Hao Li, Tiehu Li

The State Key Laboratory of Solidification Processing, Northwestern Polytechnical University, Xi’an 710072, China;
*E-mail: jixianglinnwpu@outlook.com, ztk@nwpu.edu.cn

Received: 28 September 2016 / *Accepted:* 9 January 2017 / *Published:* 12 February 2017

Chitosan oligosaccharide (COS)/multi-walled carbon nanotube (MWCNT) composite was prepared by electrostatic self-assembly method. The thickness of COS uniformly enwrapped on the surface of MWCNTs is around 3.3 nm. COS/MWCNT composites exhibit excellent electrochemical property in 1mM $[Fe(CN)_6]^{3-/4-}$ solution. The results showed that the composites with 10 wt % MWCNTs presented obvious redox peak and low impedance and have good electrochemical response. The redox peak currents were linear while the concentration of copper sulfate ranging from 2×10^{-8} to 2×10^{-6} M. The relationship between oxidation peak currents I(A) and Cu^{2+} concentration C (M) is: i_{pk} (A) = 2.228 $\times 10^{-6}$ + 12.96*C (M)，

Keywords: chitosan oligosaccharide (COS), multi-walled carbon nanotubes (MWCNTS), electrochemical properties, copper ion

1. INTRODUCTION

Chitosan oligosaccharide(COS) is derivatives of chitin material, a kind of polysaccharide containing multiple amino. Its chemical structure is similar with plant fiber and it is only the alkalinity small molecules with positive charge in natural polysaccharides. COS has stable three-dimensional structure and its ring can chelate bivalent heavy metal ion. COS has very strong absorbability and it can combine with a variety of poisonous metal, nonmetal and toxin (including cancer toxin). It has been widely used in biomaterial and medicine & health products [1] because of its special physiological activity and water-solubility. Yong [2] has compared the adsorption effect of nine series of oligosaccharide/chitosan derivatives as adsorbents for the same concentration of lead ion. They also discussed the adsorbing competition among lead, cadmium and chromium metal ions, and the results showed that the adsorbing effect is the most important for cadmium and lead which can reach to 80%.

Chitosan and its derivatives have an widely use in biological medicine, fine chemical industry and environmental protection [3] .The short-chain structure, low viscosity, and good solubility in water make the COS better than chitosan in many aspects. In recent years, COS has drawn more attention of many researchers. Carbon nanotubes (CNTs) with unique electronic properties can promote electronic transmission while they were made electrodes [4,5,6]. The physicochemical properties of CNTs such as porosity, large specific surface area and various functional groups which were introduced by functional modification are very important for the electrode interface so that presenting unique catalytic effect towards the electrochemical behaviors of certain materials. There are quantities of researches focusing on the application [21-25] of CNTs as sensor base material. The adding of MWCNTs makes Carbon paste electrode show better performance in comparison with traditional carbon paste electrodes, improving the detection limit, lifetime, response time, dynamic working range, and stability of the nano-composite sensor due to its high conductivity [21]. Besides, M. Soleimani et. al’s research indicating that MWCNTs are incorporated into the composition of electrode to decrease the ohmic resistance and MWCNT modified the potentiometric carbon paste electrodes are good analytical tools for copper ion determinations [24]. P. Norouzi et. al show that the pastes prepared using functionalized multi-walled carbon nanotube, nanosilica, graphite, and room temperature ionic liquid have a long-term stable electrode for potentiometric uses [23]. F. Faridbod et. al show that the carbon paste made based on a new nano-composite including multi-wall carbon nanotube, and room temperature ionic liquid showing better sensitivity, selectivity, response time, response stability and lifetime in comparison with typical carbon paste electrodes [25].

Although the investigations of COS used in biomedical field [7,8] are abundance, the up-to-date literatures studied the electrochemical properties of COS/MWCNT composite are few. Based on our previous works, COS/MWCNT composite were synthesized and the electrochemical properties were also studied.

2. EXPERIMENTAL

2.1 Materials

MWCNTs with 95% purity were supplied by Beijing Nano Technology LTD.(Beijing, China). COS (molecular weight: 1000～2000 and 3000～5000, 98% deacetylation) was purchased from Xi’an LiFei Technology LTD.(Xi’an, China). Nitric acid (analytical purity, 65～68%) and sulfuric acid (analytical purity, 95～98%) were purchased from Tianjin Third Chemical Factory(Tianjin, China). Phosphate buffer solution (PBS, pH6.9) was prepared for electrochemical measurement. Other chemicals were of analytical grade and used as original received. All aqueous solutions were prepared using deionized water.

2.2 Characterization

The surface morphology of COS/MWCNT composite was investigated by field-emission scanning electron microscope (FE-SEM) at an accelerating voltage of 10 kV. High resolution transmission electron microscopy (HR-TEM) was conducted with JEOL JEM-3010 at an accelerating voltage of 300 kV. The crystal structures of the samples were analyzed by an Xray powder diffractometer (XRD; D/Max 2500 V PC^{-1}, Cu-Ka radiation). Electrochemical properties (DPV, CV, AC impedance) were measured using a Electrochemical workstation with a three-electrode system which was composed of either a GC electrode or a GC electrode coated with a COS/MWCNT composite as the working electrode, a saturated calomel electrode (SCE) as the reference electrode and a Pt wire as the counter electrode.

2.3 Preparation

The MWCNTs were treated by concentrated sulfuric acid and concentrated nitration acid with a ratio of 3:1 for the introduction of carboxylic acid groups. 2g chitosan oligosaccharide was dissolved in deionized water and treble the water volume of alcohol was added to precipitate the chitosan oligosaccharide. This process is to remove the impurity in the chitosan oligosaccharide.

A certain amount(0.05g, 0.1g, 0.2g, 0.45g, 0.95g) of COS was dissolved in deionized water by ultrasonication for 30 *min*, then mixed with 50 ml of $1mg·mL^{-1}$ COOH-MWCNTs solution. The blended solution was stirred for 4*hrs*. Diluted ammonia solution was added dropwise to the MWCNTs–COS dispersions. With increasing of the pH value of the system, the ionized chitosan oligosaccharide would be deionized and become non-dissolvable in aqueous media, and thus these adsorbed as well as the soluble chitosan oligosaccharide deposit on the surface of carbon nanotubes forming a layer of chitosan coating.The GC electrode was polished using 0.3 and 0.05 um alumina slurry in sequence and ultrasonicated with acetone ,ethanol and deionized water for 3 min respectively. This solution was deposited on the clean surface of GC electrode using a micro syringe, and finally dried with an infrared lamp to obtain a finished GC electrode coated with MWCNTs/COS composite [9].

3. RESULTS AND DISCUSSION

3.1 XRD diffraction spectra

Figure 1 shows the X-ray diffraction (XRD) patterns of COOH-MWCNTs and MWCNTS/COS composite. Figure 1a is the diffraction diagram of the mixed acid treated MWCNTs. It shows that there is a strong peak corresponding to (002) (d = 3.477), which is more obvious than that of graphite (d=3.331). There are also three peripheral peaks corresponding to the (100), (004) and (110) crystal planes of graphite, and the d values are 2.1076, 1.7188 and 1.2258, respectively. This shows that the purity of MWCNTs is higher after the treating of mixed acid (HNO_3:H_2SO_4=1:3, V/V), and MWCNTs no longer contain amorphous carbon and other metals.

Figure 1b shows the XRD pattern of COS/MWCNTs composite. Chitosan oligosaccharide has diffraction peaks at 10 ° and 20°, which can be attributed to the amino and hydroxyl of hydrogen bond. The peaks of the composite are similar to neither MWCNTs nor COS, which indicates that maybe there is some interaction between MWCNTs and COS.

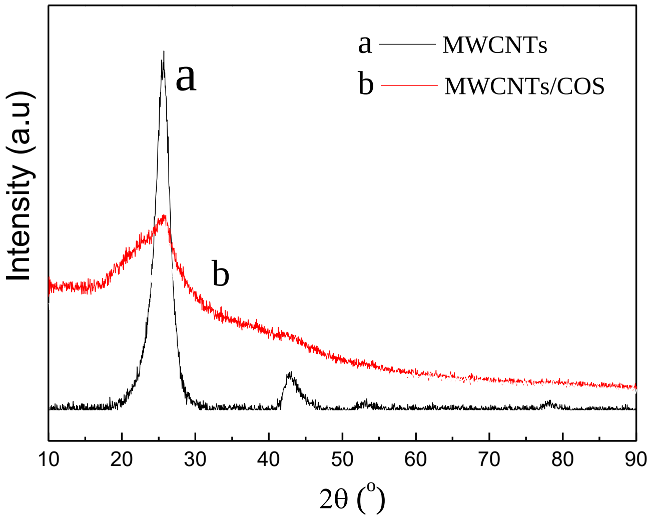

Figure 1. XRD pattern of MCNTS(a) and COS/MCNTS composite(b)

3.2 Electron imaging analysis.

An FE-SEM image of COOH-MWCNTs is shown in Figure 2a, which indicates that most of MWCNTs are tangled together and the surface is smooth and the diameters are about 10 nm to 20 nm. Figure 2b,c, and d is for the COS modified MWCNTs, which shows that the morphology of MWCNTs/COS composite is still tubular but rough and the diameter reaches 80 nm. This shows that COS are coated on the surface of MWCNTs under ultrasonication.

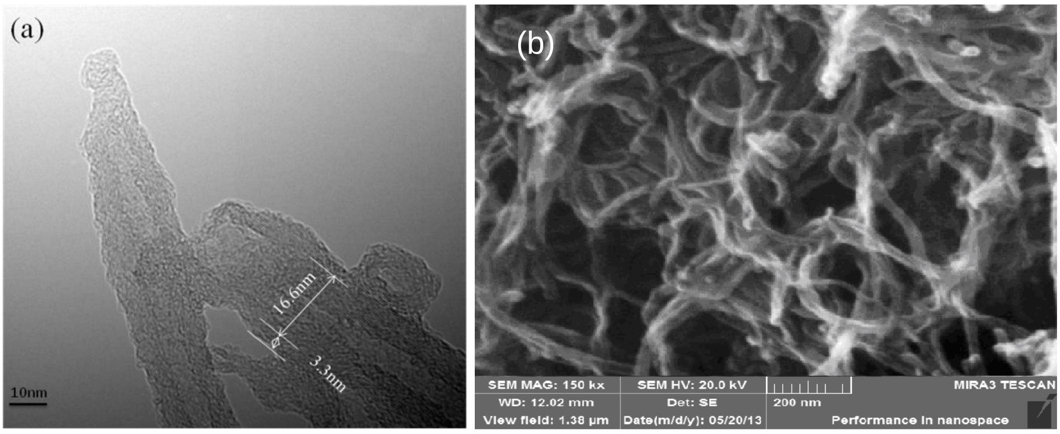

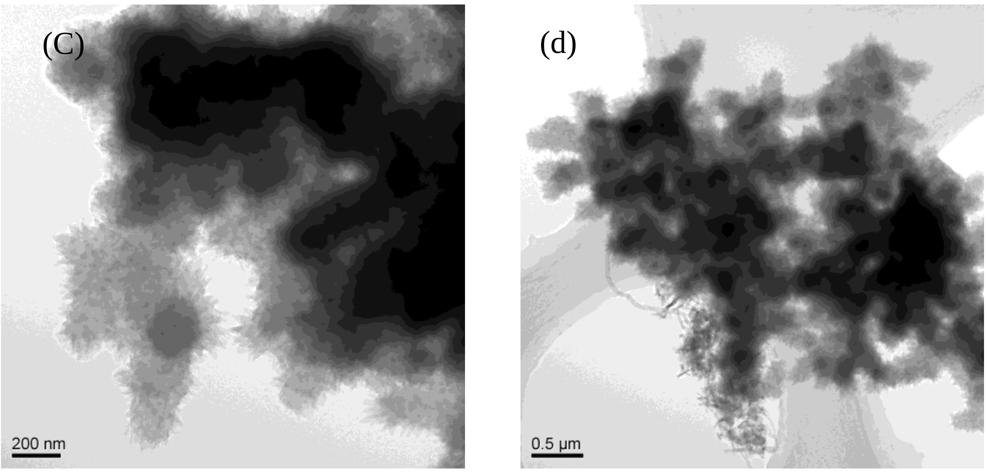

Figure 2. FE-SEM image(a) of MCNTS, COS/MCNTS composite(b). TEM image of COS/MCNTs composite(c,d)

3.3 Electrochemical characteristics of GC electrode coated with MWCNTs/COS composites at different contents of MWCNTs.

Figure 3 shows the cyclic voltammograms(CVs) of different GC electrodes in 1mM $[Fe(CN)_6]^{3-/4-}$ pH 6.9 PBS solution containing 0.1 M KCl at a scan rate of 0.02V/s. It shows that the oxidation peak is the lowest for pure COS while the oxidation peak is obvious when the content of MWCNTs is 10 wt%. This is due to the synergistic effects of the molecular wire effect of MWCNTs and a large number of amino groups in COS molecules which can chelat and capture many ions. The surface porous structure of the composite is in favor of small molecule’s absorption and dispersion.

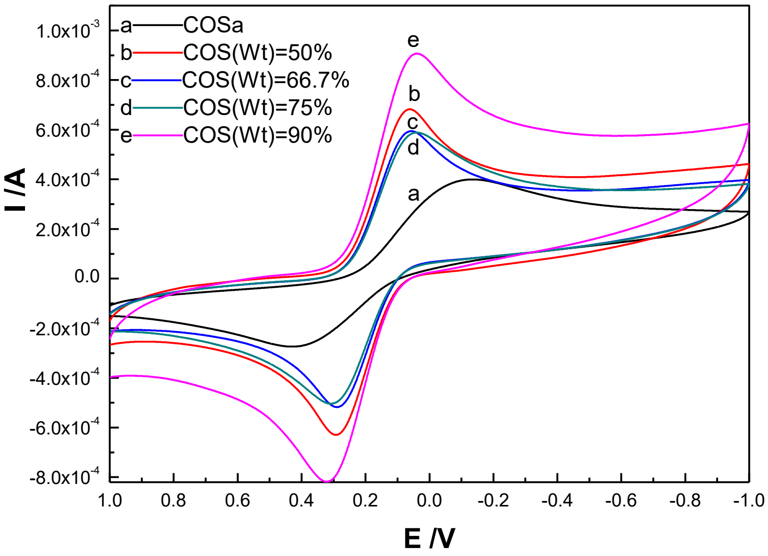

Figure 3. CVs of GC electrode in 1mM [Fe(CN)6]3-/4-(scan rate:0.02V/s). Electrode materials of (a) pure COS (b) 50 wt% COS (c) 66.7 wt% COS (d) 75 wt% COS (e) 90 wt% COS

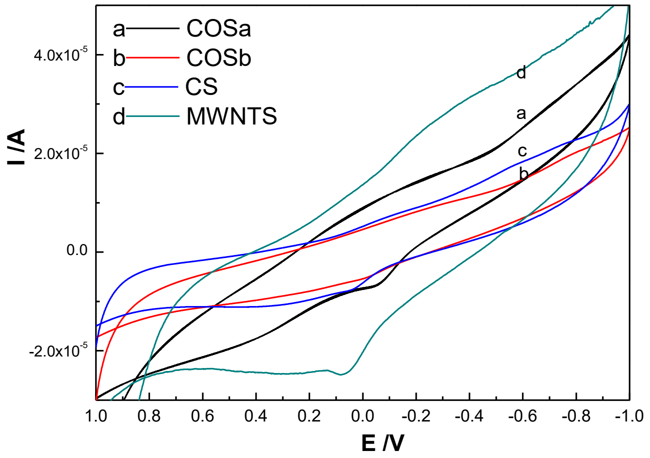

Figure 4. CVs of the different electrodes : a, COSA(Relative molecular mass 1000~2000)； b，COSB(Relative molecular mass 3000~5000) ; c, CS ; d ,MWNTS in 10^{-8}M/L $CuSO_4$ solution.

Figure 4 shows the CVs of the GCE coated with different materials in 10^{-8}M $CuSO_4$ solution. It indicates that there merely does not exist a redox peak in CV of the GCE coated with COS with molecular weight 3000 ~ 5000. However, there exists an obvious redox peak at -0.057 V in the CV of the GCE coated with molecular weight 1000~2000. This may be because COS with short chain has a larger specific surface area, thus having more space to adsorb and capture copper ions.

Figure 5 shows the CVs of composites modified glassy carbon electrode with different contents of MWCNTs in 10^{-8}M $CuSO_4$ solution. It indicates that the redox peaks of all MWCNTs/COS are obvious. And it shows that the redox peak is the highest when the content of MWCNTs is 10%. This is due to the synergistic effects of the molecular wire effect of MWCNTs and a large number of amino groups in COS molecules which can chelat and capture many ions.

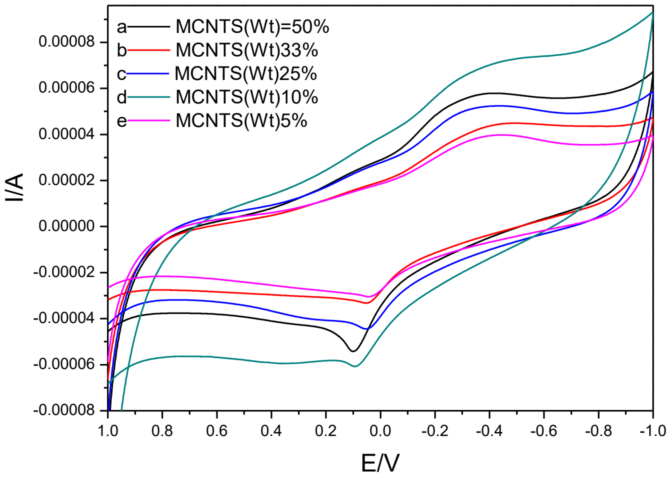

Figure 5. CVs of GCE coated with different electrodes : a, COSA(Relative molecular mass 1000~2000) ； b ， COS/MWNTS=1:1; C,COS/MWNTS=2:1; d ， COS/MWNTS=4:1; e,COS/MWNTS=9:1 in 10^{-8}M/L $CuSO_4$ solution.

Figure 6 shows CVs of the GCE coated with the COS/MWNTS composite with 10% MWCNTs in 10^{-8} M $CuSO_4$ solution at different scan rates. The redox peak currents improved with the increasing of scan rates. It implied that the GCE coated with the COS/MWNTS composite has a good electrochemical response in Cu^{2+} solution.

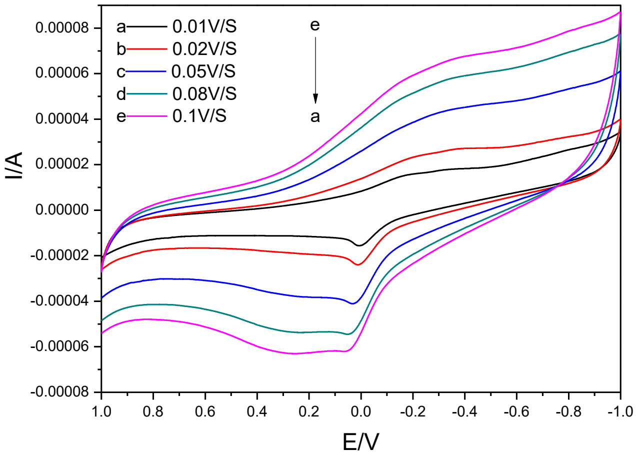

Figure 6. CVs of GCE coated with COS/MWCNT composite in 10^{-8}M/L $CuSO_4$ solution(PH4.5) at various scan rates:a,0.01V/S; a,0.02V/S; a,0.05V/S; a,0.08V/S; a,0.1V/S.

.

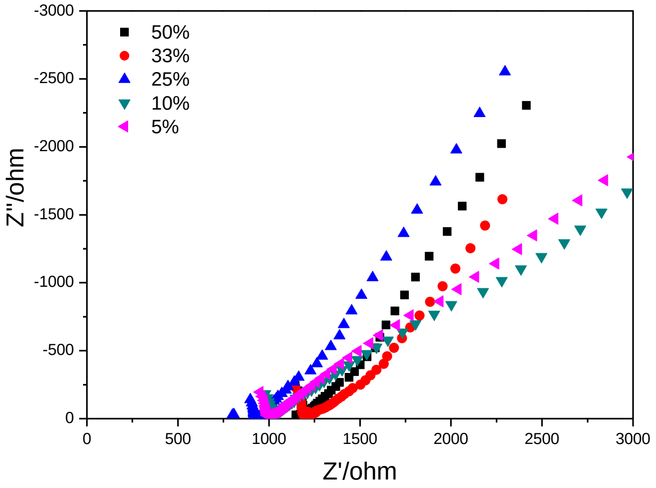

Figure 7. AC impedance plots of the GC electrode with different contents of CNTs (a) 50 wt% (b) 33 wt% (c) 25 wt% (d) 10 wt% (e) 5 wt% coated with COS/MCNTS

Figure 7 shows the AC impedance plots of the GC electrode coated with the MWCNTs/COS composites with different contents of MWCNTs in 10^{-8}M $CuSO_4$ solution (pH4.5). The AC impedance spectrum is composed of a semicircle at high frequencies and a inclined line at low frequencies. The semicircle at high frequencies is related to the electron-transfer kinetics of the redox probe on the electrode surface and the diameter represents the charge transfer resistance and the linear part at lower frequencies corresponds to surface diffusion control process [10, 13, 14]. In Figure 7, the impedance spectrum in the high frequencies approximates a straight line, which indicates that the electron transfer resistance of the MWCNTs/COS composite is very small. It may be due to the porous structure of the composite. And the radius is the smallest when the content of MWCNTs is 10%, thus indicates that 10% is the proper proportion to promote the electron transmission, which is in accordance with other researchers' reports on CNTs-decorated electrode [11, 15].

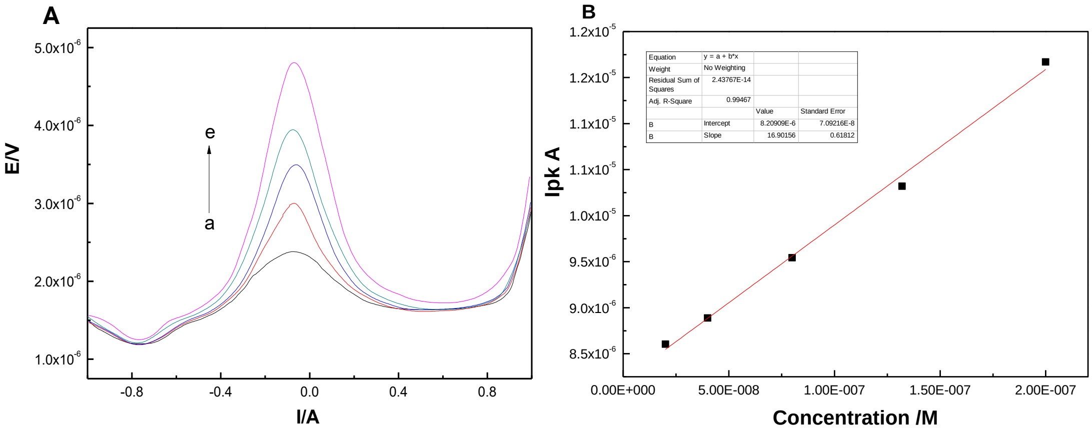

Equation	y = a + b*x		
Weight	No Weighting		
Residual Sum of Squares	2.43767E-14		
Adj. R-Square	0.99467		
		Value	Standard Error
B	Intercept	8.20909E-6	7.09216E-8
B	Slope	16.90156	0.61812

Figure 8. DPV curves of the GC electrode coated with a COS/MWCNT composites in linear range from 2.18×10^{-8} to 2×10^{-7}mol/L(a–e:the concentration of Cu^{2+} is 2.18×10^{-8}、4×10^{-8}、8×10^{-8}、1.32×10^{-7}、2×10^{-7}mol/L respectively), and linear relationship between redox peak and Cu^{2+} concentration.

DPV method has been used widely for the detection of heavy metal ion [11, 16]. Figure 8 shows the linear relationship between redox peak currents and Cu^{2+} concentration. The redox peak currents increased with the concentration Cu^{2+} from 2×10^{-8} mol/L to 2×10^{-7} mol/L. A linear fit of this data gives the follow equation, i_{pk} (A) = 8.209 E-6 + 16.902 C (M), where i_{pk} is the redox peak curruent and C is the Cu^{2+} concentration. The linear coefficient between currents and concentration was 0.995. Table 1 is the comparison of different copper(II) ion detection electrode materials [17-21]. Compared with other electrode materials, the MWCNTs/COS composite shows a pretty low detection limit, which might be due to the combined effects of MWCNTs and COS. Besides, this electrode material is really cost-effective and high detection efficiency.

Table 1. Comparison of different Copper(II) ion detection electrode materials

Electrode	Detection Limit (M)	Linear Range (M)	Ref
Copper Sulfide/Platinum Electrode	10^{-6}	$1\text{-}10^{-4}$	17
Screen-Printed Platinum Electrodes	10^{-6}	$4\times10^{-5}\text{-}10^{-3}$	18
Undoped Conducting Polymers	10^{-5}	$10^{-5}\text{-}10^{-3}$	19
Spiropyran Derivative	$1.5*10^{-7}$	$7.5\times10^{-7}\text{-}3.6\times10^{-5}$	20
MWCNTs/COS composite	2.18×10^{-8}	$2\times10^{-8}\text{-}2\times10^{-7}$	Ours

4. CONCLUSIONS

A MWCNTs/COS composite was prepared using in-situ synthesis. COS can be coated on the surface of MWCNTs uniformly and it can effectively improve the dispersion of MWCNTs. MWCNTs/COS has a good electrochemical response in $[Fe(CN)_6]^{3-/4-}$ solution. When the content of MWCNTs was 10%, COS could be more evenly wrapped on the surface of MWCNTs. The MWCNTs/COS composite had better electrochemical catalysis towards Cu^{2+} than pure COS. The MWCNTs/COS composite has certain detection ability for Cu^{2+} concentration and has a good stability and repeatability.

ACKNOWLEDGMENTS
This work was supported by the Specialized Research Fund for the Doctoral Program of Higher Education (20096102120016), Natural Science Foundation of China (51572221, 51672221), China Aeronautical Science Fund (2014ZF53074), the Key Science and Technology Program of Shaanxi Province, China (2013K09-03), and the “111” Project (B08040).

References

1. L. Lillo, J. Alarcón, G. Cabello, C. Céspedes, and C. Caro, *Z. Naturforsch*., 63 (2008) 644-648.
2. S. K. Yong, N. S. Bolan, E. Lombi, and W. Skinner, *Crit. Rev. Env. Sci. Technol*., 43 (2012) 1741-1794.
3. K. Kurita, *Polym. Degrad. Stab*., 59 (1998) 117-120.
4. V. Khalili, J. Khalil-Allafi and W. Xia, *Appl. Surf. Sci*., 366 (2016) 158-165.
5. S. Liu, Y. H. Sun, F. C. Zhou, and J. M. Nan, *Appl. Surf. Sci*., 375 (2016) 101–109.
6. D. Janas, K. K. K. Koziol, *Appl. Surf. Sci*., 376 (2016) 74-78.
7. M. Dash, F. Chiellini, R. M. Ottenbrite, and E. Chiellini, *Prog. Polym. Sci*., 36 (2011) 981-1014.
8. R. Jayakumar, M. Prabaharan, S. V. Nair and H. Tamura, *Biotechnol. Adv*., 28 (2010) 142-150.
9. Y. Liu, J. Tang, X. Q. Chen and J. H. Xin, *Carbon*., 43 (2005) 3178-3180.
10. Y. Liu, H. Y. Gu, *Microchim. Acta*., 162 (2008) 101-106.
11. H. Xu, L. P. Zeng, S. J. Xing, Y. Z. Xian, G. Y. Shi and L. T. Jin, *Electroanalysis*., 20 (2008) 2655-2662.
12. J. Morton, N. Havens, A. Mugweru, A. K. Wanekaya, *Electroanalysis*., 21 (2009) 1597-1603.
13. C. Y. Xiong, T. H. Li, T. K. Zhao, Y. D. Shang, A. L. Dang, X. L. Ji, H. Li and J. G. Wang, *Electrochim. Acta*., 217 (2016) 9-15.
14. C. Y. Xiong, T. H. Li, A. L. Dang, T. K. Zhao and H. Q. Lv, *Rsc. Adv*., 5 (2016) 602-610.
15. B. Feier, I. Bajan, I. Fizesan, D. Floner, C. Cristea, F. Geneste and R. Sandulescu, *Int. J. Electrochem. Sci*., 10 (2015) 121-139.
16. B. B. Prasad, S. Fatma, *Sen Actuators, B Chem*., 229 (2016) 655-663.
17. M. Kupper, J. W. Schultze, *J. Electroanal. Chem*., 427 (1997) 129-35.
18. A. Cranny, N. R. Hamis, M. Nie and J. A. Wharton, *IEEE Sens. J*., 12 (2012) 2091-2099.
19. R. Prakash, R. Srivastava, P. Pandey, *J. Solid State Electrochem*., 6 (2002) 203-208.
20. N. Shao, Y. Zhang, S. M. Cheung, R. H. Yang, W. H. Chan, T. Mo, K. A. Li, F. Liu, *Anal. Chem*., 77 (2005) 7294-7303.
21. M. R. Ganjali, Z. Rafiei-Sarmazdeh, T. Poursaberi, *Int. J. Electrochem. Sci*, 7 (2012) 1908-1916.
22. N. Ghorbani, S. Hosseinzadeh, S. Pashaei, *Int. J. Electrochem. Sci*, 9 (2014) 7574-7586.
23. P. Norouzi, M. Pirali-Hamedani, S. O. Ranaei-Siadat, *Int. J. Electrochem. Sci*, 6 (2011) 5189-5199.
24. M. Soleimani, M. G. Afshar, *Int. J. Electrochem. Sci*, 8 (2013) 8719-8729.

25. F. Faridbod, M. R. Ganjali, M. Pirali-Hamedani, *Int. J. Electrochem. Sci*, 5 (2010) 1103-1112.